International Journal on Recent and Innovation Trends in Computing and Communication
ISSN: 2321-8169 Volume: 11 Issue: 9
Article Received: *25 July 2023* ***Revised:*** *12 September 2023* ***Accepted:*** *30 September 2023*

Calculus-Based Model of Temperature and Velocity with Convective Boundary Conditions Method of Homotopy Analysis

Mamatha J
Designation: Assistant Professor of Mathematics
College: Govt. First Grade College for Women, Vijayanagara, Mysuru – 570032
Email id: mamatha.j749@gmail.com

Abstract

The goal of this work is to provide a mathematical model for the study of temperature and velocity partial differential equations with convective boundary conditions. The nonlinear partial differential equation that governs is solved using the Homotopy Analysis Method. Plotting temperature and velocity on a graph allows one to examine the behaviors of the various factors. We analyze and provide in tabular form the impact of skin friction and the local Nusselt number on different parameters.

Keywords: *Skin friction, Homotopy Analysis Method, Boundary Conditions, Casson Fluid, and mathematical modeling.*

Introduction

In many industrial and real-world situations, there exist flows that are triggered not only by variations in temperature but also by variations in concentration. These variations in mass transfer have an impact on the pace of heat transmission. Numerous industrial transport procedures include the transmission of mass and heat. In many chemical processing sectors, including the food and polymer industries, heat and mass transfer are typical occurrences. Free convection fluxes are of relevance to many industrial applications, including granular and fiber insulation, geothermal systems, and so on [1].

The effects of radiation heat on a number of fluid flow models were investigated by Ibrahim et al. [2] and Aliakbar et al. [3]. For many technical uses, convective heat transfer in nanofluid flow is essential. Das [4] examined the flow and heat transfer of a Cu-water nanofluid in a mixed convection stagnation point in the direction of a diminishing sheet. Chaudhary and Merkin [5] examined homogeneous-heterogeneous responses in boundary layer flow. Around the two-dimensional stagnation point flow, Khan and Pop [6] studied the flow effects on an infinite permeable wall with homogeneous-heterogeneous responses. The continuous MHD boundary layer flow of electrically conducting Casson fluid past an increasingly decreasing shrinking sheet was studied by Mahanta [7].

Mukhopadhyay [8] talked on the impact of heat transfer past a stretched surface and slip-on unstable mixed convective flow. Heat and mass transmission in a vertical plate of laminar free convection boundary-layer flow were studied simultaneously by Lin and Wu [9]. Bhattacharya et al. [10] looked at the analytical solutions for the heat transfer towards the decreasing sheet and the boundary layer stagnation point flow. The magnetohydrodynamic flow of a viscous incompressible fluid caused by surface deformation was studied by Pavlov [11].

Wang [12] investigated the three-dimensional flow produced by a stretched flat surface. Cross-mass transfer phenomena in a lower stretched wall channel were studied by Mehmood and Ali [13]. [14] looked at the mass transfer mechanisms in a channel flow across a stretched surface.

In this study, the homotopy analysis technique (HAM) is utilized to derive an analytical equation for the temperature profile and concentration velocity. In addition, the local Nusselt number and the Skin Friction analytical solution are investigated. The HAM's auxiliary parameter h causes the analytical solution to converge. It illustrates the behavior of each parameter.

Mathematical Formulation

Think about the three-dimensional (3D) incompressible flow across a stretched sheet. While fluid is introduced into the z-axis, the sheet is stretched in the xy-plane.

International Journal on Recent and Innovation Trends in Computing and Communication
ISSN: 2321-8169 Volume: 11 Issue: 9
***Article Received:** 25 July 2023 **Revised:** 12 September 2023 **Accepted:** 30 September 2023*

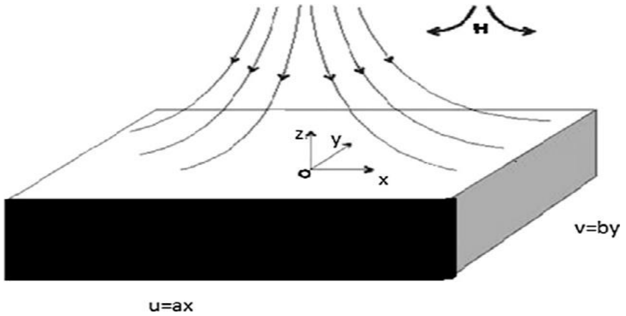

Fig.1. Physical model and coordinate systems [7].

The following is an introduction to the dimensionless variables for the concentrations in the equations that link the nonlinear differential equations to the dynamic circumstances [7]:

$$\left(1+\frac{1}{\beta}\right) F''' - (F')^2 - (F + c\,G)F'' - (M^2+\lambda)F' = 0 \quad (1)$$

$$\left(1+\frac{1}{\beta}\right) G''' - (G')^2 - (F + c\,G)G'' - (M^2+\lambda)G' = 0 \quad (2)$$

$$(1+R)\,\phi'' + P_r(F + c\,G)\phi' = 0 \quad (3)$$

where M^2 is the magnetic parameter, P_r is the Prandtl number, λ is the porosity parameter, R is the radiation parameter, Biot number (B_i)and stretching parameter (c).

The following boundary conditions are

$$\eta = 0: \; F(0) = 0, G(0) = 0, F'(0) = 1, G'(0) = c, \phi'(0) = -B_i(1-\phi(0)) \quad (4)$$

$$\eta = \infty: \; F'(\infty) = 0, G'(\infty) = 0, \phi(\infty) = 0 \quad (5)$$

1. Homotopy Analysis Method: Analytical Solutions for the Velocities and Temperature

A semi-analytical method for resolving nonlinear issues is homotopy analysis. This method was originally proposed by Liao [15]. Unlike other analytical approaches, this method is independent of small/large physical characteristics. A straightforward technique for guaranteeing solution series convergence in a limited number of iterations is the Homotopy Analysis Method. The following approximate analytical formulations were produced by applying the Homotopy Analysis Method to solve the nonlinear equations (2) through (6):

$$F(\eta) = \frac{1}{\sqrt{s}}\left(1 - e^{-\sqrt{s}\,\eta}\right) + \frac{h(c^2+2)}{6s\sqrt{s}}\left[e^{-2\sqrt{s}\,\eta} - 2e^{-\sqrt{s}\,\eta} + 1\right] + \frac{5k(h-h^2)(M^2c^2+2M^2+\lambda c^2+2h) - h^2kc^2(10-3c^2) - 3h(1+c^2)(m^2+\lambda)}{18s^2\sqrt{s}}\left[1 - 2e^{-\sqrt{s}\,\eta} + e^{-2\sqrt{s}\,\eta}\right] + M\,\frac{(c^2+2)[4(h-h^2)(m^2+\lambda) - 2h^2(1+c^2)]}{6s^2} + \frac{h^2(c^2+2)(c^2+3)}{36s^2\sqrt{s}}\left[2 - 3e^{-\sqrt{s}\,\eta} + e^{-3\sqrt{s}\,\eta}\right] \quad 6)$$

$$G(\eta) = \frac{c}{\sqrt{s}}\left(1 - e^{-\sqrt{s}\,\eta}\right)\frac{h(c^3+2c)}{6s\sqrt{s}}\left[e^{-2\sqrt{s}\,\eta} - 2e^{-\sqrt{s}\,\eta} + 1\right] + \frac{5k(h-h^2)(M^2c^3+2M^2c+\lambda c^3+2hc) - h^2kc^3(10-3c^2) - 3h(c+c^3)(m^2+\lambda)}{18s^2\sqrt{s}}\left[1 - 2e^{-\sqrt{s}\,\eta} + e^{-2\sqrt{s}\,\eta}\right] + M\,\frac{(c^3+2c)[4(h-h^2)(m^2+\lambda) - 2h^2(1+c^2)]}{6s^2} + \frac{h^2c\,(c^3+2c)(c^2+3)}{36s^2\sqrt{s}}\left[2 - 3e^{-\sqrt{s}\,\eta} + e^{-3\sqrt{s}\,\eta}\right] \quad (7)$$

$$\phi(\eta) = \frac{B_i(1+R)}{G+B_i(1+R)}\,e^{-\left(\frac{G}{1+R}\right)\eta} \quad (8)$$

where $s = \frac{M^2+\lambda}{k}, k = 1+\frac{1}{\beta}, G = \frac{P_r(1+c^2)}{\sqrt{s}} + \frac{h(c^2+2)(1+c)}{6s\sqrt{s}}, M\,\frac{e^{-\sqrt{s}\,\eta}-1}{\sqrt{s}} + xe^{-\sqrt{s}\,\eta}$

The dimensionless local Nusselt number and skin friction are as follows for analytical expressions [7]:

$$Re_x^{1/2}C_{fx} = \left(1+\frac{1}{\beta}\right)F''(0) \quad (9)$$

$$Re_x^{1/2}C_{fy} = \left(1+\frac{1}{\beta}\right)F''(0) \quad (10)$$

where $C_{fx} = \frac{\tau_{wx}}{\rho u_w^2}, \quad C_{fy} = \frac{\tau_{wy}}{\rho u_w^2}$

C_f is the skin friction, C_{fx} and C_{fy} are skin friction along the x- and y-directions τ_{wx} and τ_{wy} are defined.

$$Re_x^{-1/2}\,Nu = -\,\phi(0) \quad (11)$$

where $Re_x = u_x(x)\,x/v$ is defined.

1. Result and Discussion

Equations (1) through (5) show how velocities and temperature are expressed analytically. This article has examined the temperature and velocity profiles for a range of physical parameter values, including M, \lambda, \beta, B_i, P_r, R, and C. The acquired analytical findings for different parameter values are shown in Figs. 2 through 10. It is in good agreement with both the numerical result [7] and the previous result.

Figures 2 through 4 show the fluid velocity for different parameter values. Fig. 2 illustrates how the velocity F^\prime(\eta) loses effect when the casson parameter increases. Figure 3 illustrates how the velocity drops as the parameter is raised. Fig. 4 shows the effects of parameters M and C on the velocity profiles. As M and C grow, the fluid velocity F^\prime(\eta) falls, as seen in the graph. Analyze the velocity profile for different values of the parameters lambda and beta in Figures 5 and 6. It is noted

International Journal on Recent and Innovation Trends in Computing and Communication
ISSN: 2321-8169 Volume: 11 Issue: 9
***Article Received:** 25 July 2023 **Revised:** 12 September 2023 **Accepted:** 30 September 2023*

that the velocity profile G^\prime(\eta) improves when the parameters \lambda and \beta are decreased. Fig. 7 illustrates how M and C affect the velocity profiles. It is observed that M grows as the fluid's velocity G^\prime(\eta) decreases.

It is clear that when parameter C grows, so does the velocity profile G^\prime(\eta). To investigate the impacts of P_r on temperature \phi(\eta), it is depicted in Fig. 8. It is evident that the parameter P_r lowers as temperature \phi(\eta) rises. Figure 9 displays the temperature profile \phi(\eta) as a function of the different values of the parameters B_i. This is because the temperature \phi(\eta) grows together with the parameter B_i. Figure 10 makes it clear that the temperature profile \phi(\eta) grows in step with the parameter R.

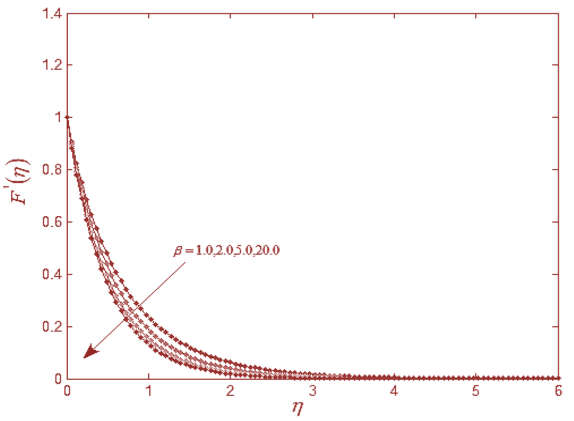

Fig.2. Analytical expression of dimensionless concentration in velocity $F'(\eta)$versus η at various values of β for fixed values of parameters $M=2, C=0.5, \lambda=0.5, h=-0.1$

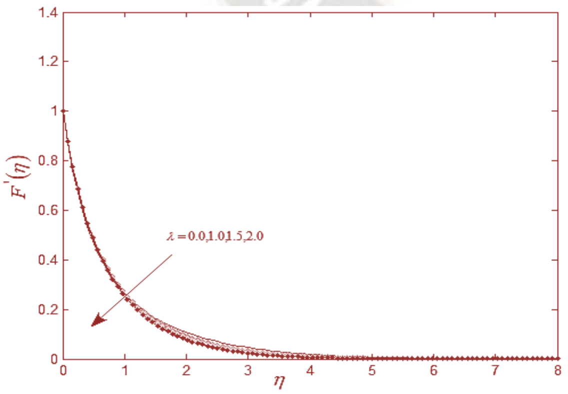

Fig.3. Analytical expression of dimensionless concentration in velocity$F'(\eta)$versusη at various values of λ for fixed values of parameters $M=2, C=0.5, \beta=0.5, h=-0.1$

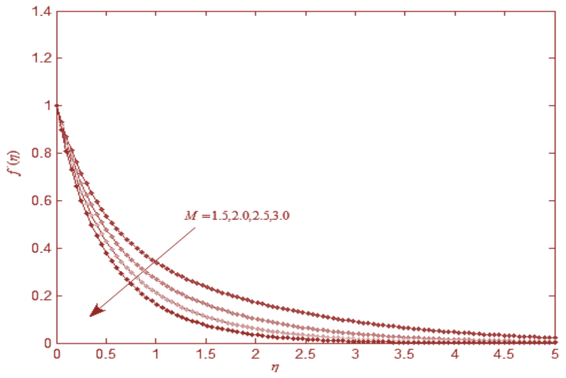

Fig.4. Analytical expression of dimensionless concentration in velocity$F'(\eta)$versusη at various values of M for fixed values of parameters $\lambda=0.5, C=0.5, \beta=0.5, h=-0.1$

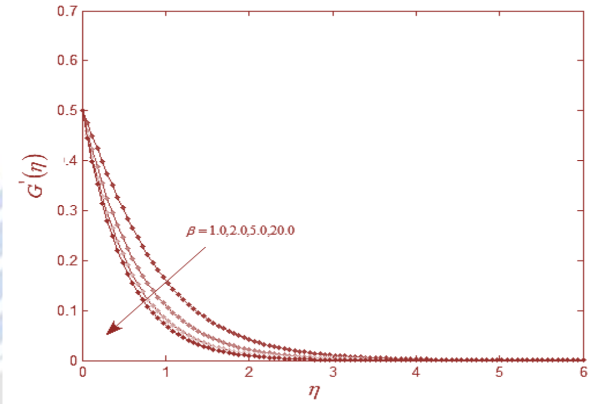

Fig.5. Analytical expression of dimensionless concentration in velocity$G'(\eta)$ versusη at various values of $\beta$for fixed values of parameters $M=2, C=0.5, \lambda=0.5, h=0.1$

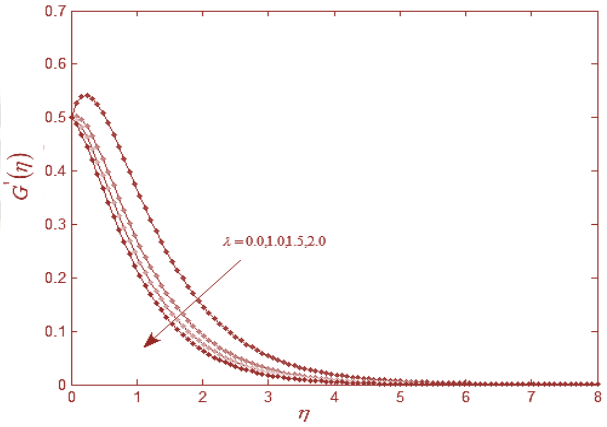

Fig.6. Analytical expression of dimensionless concentration in velocity$G'(\eta)$versusη at various values of $\lambda$for fixed values of parameters $M=2, C=0.5, \beta=0.5, h=0.1$

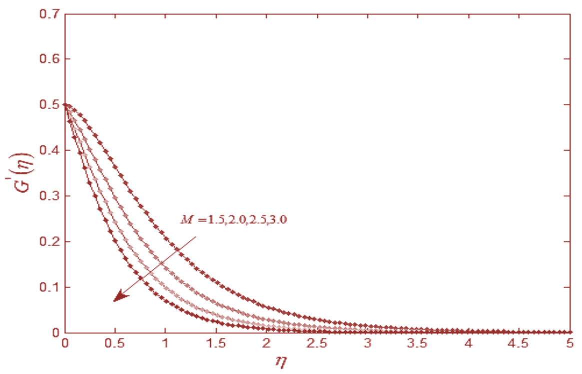

Fig.7. Analytical expression of dimensionless concentration in velocity$G'(\eta)$versusη at various values of $M$for fixed values of parameters $\lambda = 0.5, C = 0.5,\ \beta = 0.5, h = 0.1$

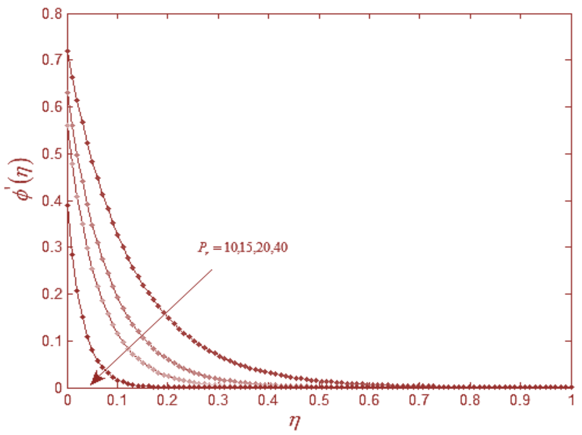

Fig.8. Analytical expression of dimensionless concentration in temperature $\phi(\eta)$versusη at various values of P_r for fixed values of parameters $M = 2, \lambda = 0.5, C = 0.5, R = 0.3, B_i = 20, \beta = 0.5, h = 0.1$

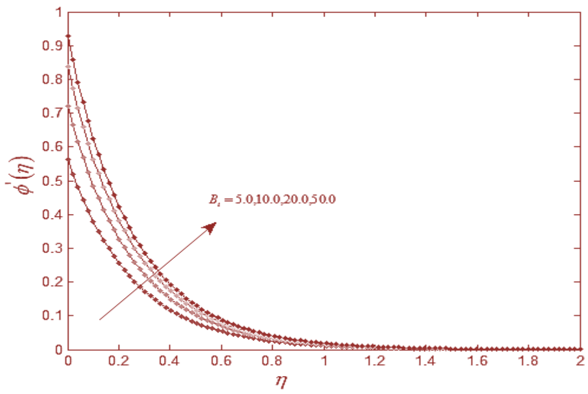

Fig. 9. Analytical expression of dimensionless concentration in temperature $\phi(\eta)$versusη at various values of B_i for fixed values of parameters $M = 2, \lambda = 0.5, C = 0.5, R = 0.3, \beta = 0.5, P_r = 5, h = 0.1$

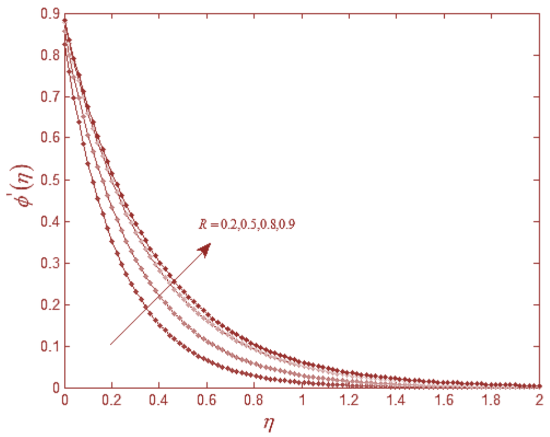

Fig. 10. Analytical expression of dimensionless concentration in temperature $\phi(\eta)$versusη at various values of R for fixed values of parameters $M = 2, \lambda = 0.5, C = 0.5,\ B_i = 20, \beta = 0.5, P_r = 5, h = 0.1$

2. Conclusion

This work presents a mathematical model of concentration in a temperature and velocity profile, which has been applied to several Casson fluid characteristics. We also looked at how many different physical characteristics affected the model's forecast. Using the Homotopy Analysis Method, the system of nonlinear partial differential equations is solved. Furthermore, impacts for different values of emerging parameters are investigated for velocities F^\prime(\eta), G^\prime(\eta), and temperature \phi(\eta). Using the Prandtl number Pr and the Lewis number\Le\ results in the opposite temperature distribution and volume fraction.

References

1. B. Awasthi, Effects of heat and mass flux on mhd free convection flow through a porous medium with radiation and first order chemical reaction, Int. J. of Applied Mechanics and Engineering, 2018, vol.23, no.4, pp.855-871.
2. F. S. Ibrahim, A. M. Elaiw, A. A. Bakr, Effect of chemical reaction and radiation absorption on the un-steady MHD free convection flow past asemi-infinite vertical permeable moving plate with heat source and suction, Comm. Nonlin. Sci. Num. Simul. 13 (6) (2008) 1056–1066.
3. V. Aliakbar, A. Alizadeh-Pahlavan, K. Sadeghy, The influence of thermal radiation on mhd flow of maxwellian fluids above stretching sheets,Communications in Nonlinear Science and Numerical Simulation 14 (3) (2009) 779–794.

4. K. Das, Mixed convection stagnation point flow and heat transfer of cu-water nanofluids towards a shrinking sheet, Heat Trans. Asian Res.42 (3) (2013) 230–242.
5. M. A. Chaudhary, J. H. Merkin, A simple isothermal model for homogeneous-heterogeneous reactions in boundary layer flow: I. equal diffusivities, Fluid Dynam. Res. 16 (1995) 311–333.
6. W. A. Khan, I. Pop, Flow near the two-dimensional stagnation point on a infinite permeable wall with a homogeneous-heterogeneous reaction,Comm. Nonliear. Sci. Numer. Simulat. 15 (2010) 3435–3443.
7. G. Mahanta, S. Shaw, 3D Casson fluid flow past a porous linearly stretching sheet with convective boundary condition, Alexandria Engineering Journal (2015) 54, 653–659.
8. S. Mukhopadhyay, Effects of slip on unsteady mixed convective flow and heat transfer past a stretching surface, Chin. Phys. B. 27 (2010) 256–307.
9. Lin H.T. and Wu C.M. (1995): Combined heat and mass transfer by laminar natural convection from a vertical plate.– Heat and Mass Transfer, vol.30, pp.369–376
10. K. Bhattacharyya, S. Mukhopadhyay, G.C. Layek, Slip effects boundary layer stagnation-point flow and heat transfer towards a shrinking sheet, J. Heat Mass Transf. 54 (2011) 308–313.
11. K. B. Pavlov, Magnetohydrodynamic flow of an incompressible viscous fluid caused by deformation of a surface, Magn. Gidrodin. 4 (1974) 146–147.
12. C.Y. Wang, The three dimensional flow due to a stretching flat surface, Phys. Fluids 27 (1984) 1915–1917.
13. A. Mehmood, A. Ali, Across mass transfer phenomena in a channel of lower stretching wall, Chem. Eng. Commun. 198 (2011) 678–691.
14. A. Mehmood, S. Munawar, A. Ali, Cooling of hot stretching surface in the presence of across mass transfer phenomena in a channel flow, Z. Naturforschung 69 (2014) 21–33.
15. S.J. Liao, “The Proposed Homotopy Analysis Technique for the Solution of Nonlinear Problems”, Ph.D.Thesis, Shanghai Jiao Tong University, 1992.